

$\text{ClO}_4^-/\text{Al-MCM-41}$ nanoparticles as a solid acid catalyst for the synthesis of 2-amino-3-cyanopyridines

Mohammad Abdollahi-Alibeik¹ · Neda Sadeghi-Vasafi¹ ·
Ali Moaddeli¹ · Ali Rezaeipoor-Anari¹

Received: 20 March 2015 / Accepted: 17 July 2015
© Springer Science+Business Media Dordrecht 2015

Abstract A one-pot four-component reaction of various types of aldehydes, acetophenone, malononitrile, and ammonium acetate was studied in the presence of perchlorated Al-MCM-41 ($\text{ClO}_4^-/\text{Al-MCM-41}$) nanoparticles for the synthesis of 2-amino-3-cyanopyridines. Mesoporous Al-MCM-41 molecular sieves with the Si/Al molar ratios of 30, 40, and 50 were synthesized by the sol-gel method and $\text{ClO}_4^-/\text{Al-MCM-41}$ with different calcination temperatures were prepared and characterized by SEM, TEM, XRD, FT-IR, potentiometric titration and, N_2 adsorption-desorption techniques. The characterization results show that $\text{ClO}_4^-/\text{Al-MCM-41}$ with calcination temperature of 300 °C has the best catalytic activity for the synthesis of 2-amino-3-cyanopyridines. The catalyst is reusable many times with moderate loss in its activity.

Keywords Nanoparticle · $\text{ClO}_4^-/\text{Al-MCM-41}$ · 2-Amino-3-cyanopyridine · Mesoporous silica · Solid acid catalyst · Multi-component

Introduction

Compounds with pyridine scaffold are known to possess a broad spectrum of biological activities such as anti HIV [1], anticonvulsant [2], anti-inflammatory [3], and antitumor [4] activity. Since the first report for the synthesis of substituted pyridine using multi-component reaction by Hantzsch [5], many synthetic methods and catalysts have been developed to improve structural features of these

✉ Mohammad Abdollahi-Alibeik
abdollahi@yazd.ac.ir; moabdollahi@gmail.com

¹ Department of Chemistry, Yazd University, Yazd 89158-13149, Iran

a Bruker D8 ADVANCE X-ray diffractometer using nickel-filtered $\text{Cu-K}\alpha$ radiation ($\lambda = 1.5406 \text{ \AA}$). The morphology was studied using a KYKY-EM3200 scanning electron microscopy. Melting points were obtained by Buchi B-540 apparatus and are uncorrected. The BET surface area was measured using a PHS-1020 (PHSCHINA) from the nitrogen adsorption–desorption isotherms at 77 K. All samples were degassed at 120 °C under flowing nitrogen for 2 h. The specific surface area (S_{BET}) was calculated from the adsorption data using the BET equation. Transmittance electron microscopy was performed with Zeiss-EM10C at 80 kV. ICP analysis was performed by VARIAN model Vista-pro instrument.

Preparation of Al-MCM-41

The synthesis of nanosized Al-MCM-41 with various Si/Al molar ratios carried out using tetraethylorthosilicate (TEOS) as the Si source, aluminium sulfate as the aluminium source, cetyltrimethylammonium bromide (CTAB) as the template and ammonia as the pH control agent with the gel composition of $\text{SiO}_2:\text{Al}_2(\text{SO}_4)_3:\text{CTAB}:\text{NH}_4\text{OH}:\text{H}_2\text{O} = 22.5:\text{X}:2.86:53.5:11555$ (X varies with the Si/Al ratio).

In a typical procedure, to a solution of CTAB (1.04 g, 2.86 mmol) in deionized water (200 ml), TEOS (5 ml) was added dropwise at 70 °C for about 30 min. The mixture was allowed to cool to room temperature and a solution of aluminium sulfate (0.109 g, 0.32 mmol) in deionized water (5 ml) was added dropwise. Then aqueous ammonia (25 wt%) was added until the pH of the solution was adjusted to 10.5 and was stirred for 12 h. The gel was separated by centrifuge and washed with distilled water (20 ml) and EtOH ($2 \times 10 \text{ ml}$), respectively. The solid was dried in an oven at 120 °C for 2 h and then calcined at 550 °C for 4 h. The obtained solid was denoted as AM-550.

Preparation of $\text{ClO}_4^-/\text{Al-MCM-41}$

$\text{ClO}_4^-/\text{Al-MCM-41}$ catalyst was prepared by mixing of AM-550 (Al-MCM-41 that template was removed at 550 °C) (100 mg) and perchloric acid (0.1 M, 2 ml). The resulting suspension was stirred at ambient temperature for 4 h. The mixture was separated by centrifuge and washed with deionized water ($2 \times 3 \text{ ml}$). The obtained solid was dried in an oven at 120 °C for 2 h to obtain perchlorated Al-MCM-41, denoted as PAM-120, and then calcined at 250, 300, 350, and 400 °C for 4 h. The obtained samples were denoted as PAM-250, PAM-300, PAM-350, and PAM-400, respectively.

General procedure for the synthesis of 2-amino-3-cyanopyridine derivatives in the presence of $\text{ClO}_4^-/\text{Al-MCM-41}$

A mixture of acetophenone (1 mmol), aldehyde (1 mmol), malononitrile (1 mmol), ammonium acetate (1.5 mmol) and catalytic amount of $\text{ClO}_4^-/\text{Al-MCM-41}$ (20 mg) was stirred under solvent-free condition at 100 °C. After completion of the reaction (monitored by TLC, eluent; *n*-hexane:EtOAc, 80:20), the catalyst was separated by

centrifuge and washed with EtOH (2×3 ml). The crude products were crystallized from EtOH and purified by column chromatography to give pure 2-amino-3-cyanopyridines.

Physical and spectroscopic data of compounds (4a-i)

2-Amino-3-cyano-4,6-diphenylpyridine (**4a**): Yellow solid, mp 186 °C (Lit. [4] 186 °C). IR (KBr) ν_{\max} (cm^{-1}): 3463 (NH_2), 3302 (NH_2), 2205 ($\text{C}\equiv\text{N}$), 1637 ($\text{C}=\text{N}$), 1573 ($\text{C}=\text{C}$). ^1H NMR (400 MHz, $\text{DMSO}-d_6$): δ (ppm) = 7.0 (s, 2H, NH_2), 7.3 (s, 1H), 7.5 (m, 3H), 7.6 (m, 3H), 7.7 (m, 2H), 8.1 (m, 2H). ^{13}C NMR (100 MHz, $\text{DMSO}-d_6$): δ (ppm) = 109.2, 117, 127.2, 128.3, 128.6, 128.7, 129.6, 130.1, 136.6, 137.5, 154.8, 158.6, 160.7, 160.8.

2-Amino-3-cyano-4-(4-methoxyphenyl)-6-phenylpyridine (**4b**): Yellow solid, mp 180–182 °C (Lit. [8] 180–182 °C). IR (KBr) ν_{\max} (cm^{-1}): 3466 (NH_2), 3308 (NH_2), 2206 ($\text{C}\equiv\text{N}$), 1639 ($\text{C}=\text{N}$), 1575 ($\text{C}=\text{C}$). ^1H NMR (400 MHz, $\text{DMSO}-d_6$): δ (ppm) = 3.8 (s, 3H, OCH_3), 6.9 (s, 2H, NH_2), 7.1 (d, 2H, $J = 8.8$ Hz), 7.3 (s, 1H), 7.5 (m, 3H), 7.7 (d, 2H, $J = 8.8$ Hz), 8.1 (m, 2H). ^{13}C NMR (100 MHz, $\text{DMSO}-d_6$): δ (ppm) = 55.3, 109.0, 114.1, 117.3, 127.2, 128.6, 129.0, 129.8, 137.6, 154.4, 158.4, 160.4, 160.88, 160.9.

2-Amino-3-cyano-4-(4-chlorophenyl)-6-phenylpyridine (**4c**): Pale yellow solid, mp 187–188 °C (Lit. [4] 188–190 °C). IR (KBr) ν_{\max} (cm^{-1}): 3486 (NH_2), 3363 (NH_2), 2216 ($\text{C}\equiv\text{N}$), 1632 ($\text{C}=\text{N}$), 1574 ($\text{C}=\text{C}$). ^1H NMR (400 MHz, $\text{DMSO}-d_6$): δ (ppm) = 7.1 (s, 2H, NH_2), 7.3 (s, 1H), 7.5 (m, 3H), 7.6 (d, 2H, $J = 8.4$ Hz), 7.7 (d, 2H, $J = 12.6$ Hz), 8.14 (m, 2H). ^{13}C NMR (100 MHz, $\text{DMSO}-d_6$): δ (ppm) = 109.1, 116.8, 127.2, 128.6, 130.3, 134.5, 135.7, 137.4, 153.0, 158.7, 160.7, 158.6, 160.8.

2-Amino-3-cyano-4-(4-methylphenyl)-6-phenylpyridine (**4d**): With solid, mp 173–174 °C (Lit. [17] 175–176 °C). IR (KBr) ν_{\max} (cm^{-1}): 3466 (NH_2), 3296 (NH_2), 2205 ($\text{C}\equiv\text{N}$), 1632 ($\text{C}=\text{N}$), 1578 ($\text{C}=\text{C}$).

2-Amino-3-cyano-6-(3,4-dimethoxyphenyl)-4-phenyl pyridine (**4e**): Yellow solid, mp 218–220 °C (Lit. [18] 212–214 °C). IR (KBr) ν_{\max} (cm^{-1}): 3512 (NH_2), 3405 (NH_2), 2199 ($\text{C}\equiv\text{N}$), 1603 ($\text{C}=\text{N}$), 1580 ($\text{C}=\text{C}$).

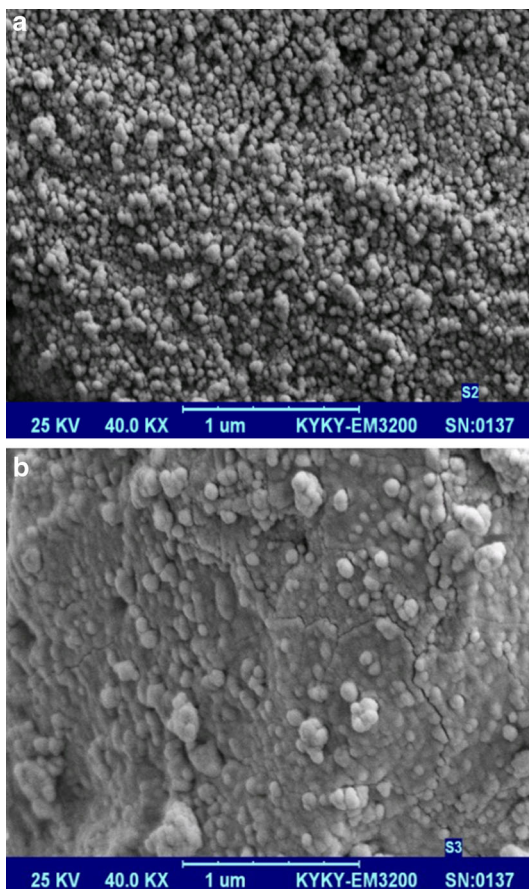
2-Amino-3-cyano-6-(3,4-dimethoxyphenyl)-4-(4-methoxyphenyl)pyridine (**4f**): Yellow solid, mp 174–176 °C (Lit. [18] 165–167 °C). IR (KBr) ν_{\max} (cm^{-1}): 3482 (NH_2), 3325 (NH_2), 2205 ($\text{C}\equiv\text{N}$), 1632 ($\text{C}=\text{N}$), 1574 ($\text{C}=\text{C}$).

2-Amino-3-cyano-6-(3,4-dimethoxyphenyl)-4-(4-chlorophenyl)pyridine (**4g**): Pale yellow solid, mp 202–204 °C (Lit. [18] 203–207 °C). IR (KBr) ν_{\max} (cm^{-1}): 3480 (NH_2), 3315 (NH_2), 2208 ($\text{C}\equiv\text{N}$), 1637 ($\text{C}=\text{N}$), 1574 ($\text{C}=\text{C}$).

2-Amino-3-cyano-6-(3,4-dimethoxyphenyl)-4-(4-hydroxyphenyl)pyridine (**4h**): Yellow solid, mp 207–209 °C (Lit. [18] 205–207 °C). IR (KBr) ν_{\max} (cm^{-1}): 3489 (NH_2), 3391 (NH_2), 2212 ($\text{C}\equiv\text{N}$), 1635 ($\text{C}=\text{N}$), 1575 ($\text{C}=\text{C}$).

2-Amino-3-cyano-6-(4-chlorophenyl)-4-(4-methoxyphenyl)pyridine (**4i**): Yellow solid, mp 200–201 °C (Lit. [19] 177 °C). 3460 (NH_2), 3367 (NH_2), 2207 ($\text{C}\equiv\text{N}$), 1608 ($\text{C}=\text{N}$), 1584 ($\text{C}=\text{C}$) (Fig. 1).

Fig. 1 SEM images of (a) AM-550 and (b) PAM-300

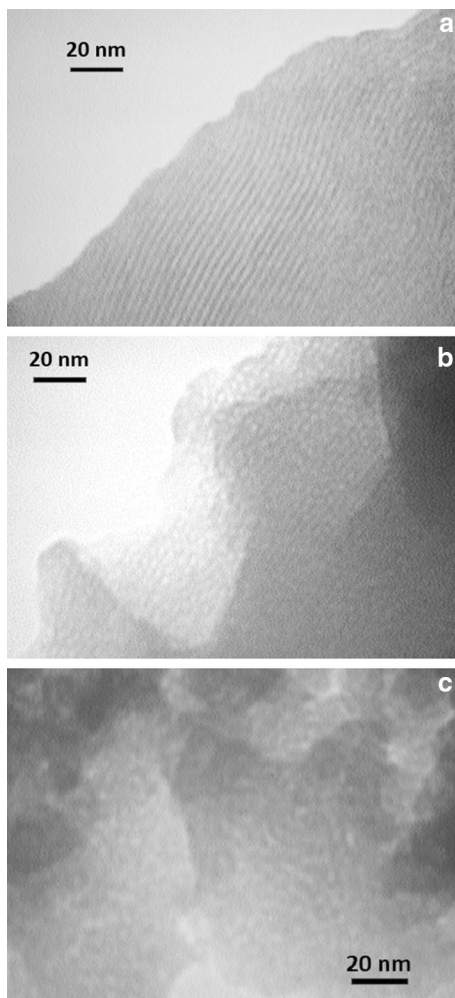


Results and discussion

Catalyst characterization

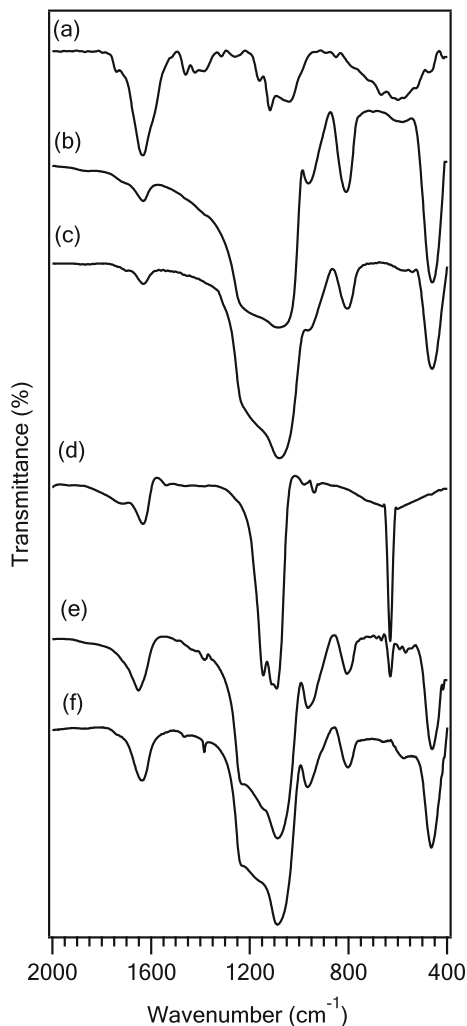
The MCM-41, AM, and PAM samples were characterized by FT-IR, SEM, and XRD techniques. The SEM images of AM-550 and PAM-300 show spherical nanoparticles with sizes of <100 nm (Fig. 1). TEM images of MCM-41, Al-MCM-41, and PAM-300 were observed in Fig. 2. As shown in Fig. 2a, the ordered mesostructure of MCM-41 as well as mesopore channels is completely obvious. Incorporation of the Al in MCM-41 lattice had not dramatic effect on the mesostructure of Al-MCM-41 (with Si/Al molar ratio of 40) (Fig. 2b). Mesostructure of the PAM-300 sample was further studied by TEM (Fig. 2c). Porosity of the catalyst is clear and pores size is observed in range of the mesoporous material (2–3 nm). Partial disarray in mesoporous structure of PAM-300 is related to the incorporation of Al into the MCM-41 framework and also acid treatment.

Fig. 2 TEM images of
(a) MCM-41, (b) Al-MCM-41
(Si/Al mol ratio of 40), and
(c) PAM-300



The FT-IR spectra of PAM-300, PAM-120, HClO_4 , AM-550, MCM-41, and Al_2O_3 are shown in Fig. 3. MCM-41 shows characteristic peaks at 460 cm^{-1} related to the bending vibration of Si–O–Si, 810 cm^{-1} relating to symmetric stretching of Si–O–Si, 960 cm^{-1} due to Si–OH and the peak at 1083 cm^{-1} relating to asymmetric stretching of Si–O–Si (Fig. 3c). The spectrum of Al_2O_3 shows corresponding peaks at 594, 1037, 1120, 1378, 1633, and 2921 cm^{-1} . The AM-550 (Al-MCM-41 calcined at 550°C) sample exhibits characteristic peaks of MCM-41. The PAM-120 sample (Fig. 3e) shows peaks of perchlorate around 630 cm^{-1} . Perchlorate peaks in the range of 933 and 1103 cm^{-1} overlap with the strong peak of MCM-41 around 960 and 1080 cm^{-1} , resulting in increase of intensity and broadening of this peak. In the spectrum of PAM-300 (Fig. 3f), the characteristic bands of perchlorate at 630 cm^{-1} disappeared, indicating the absence of free perchloric acid after calcination process. However, slight broadening of the

Fig. 3 FT-IR spectra of (a) Al₂O₃, (b) MCM-41, (c) AM-550, (d) HClO₄, (e) PAM-120, (f) PAM-300



peaks in the region of 1100–1200 cm⁻¹ confirms the presence of perchlorate in the sample. Increase in the intensity of the peak of PAM-300 at 960 cm⁻¹ compared with AM-550, may be due to increase of the number of silanol groups (Si–OH) on the surface because of the interaction of perchlorate with surface. Displacement of large aluminum atoms with small silica atoms change lattice vibration bands to lower wavenumber at 1168 and 1180 cm⁻¹. The peak at 1635 cm⁻¹ in all of samples is assigned to bending vibration of HOH due to the presence of water on the pellet samples.

The low-angle XRD patterns of MCM-41, Al-MCM-41, and ClO₄⁻/Al-MCM-41 are shown in Fig. 4. The MCM-41 pattern shows characteristic peaks at 2θ = 2.42°, 4.24°, 4.74°, and 6.18°. The XRD patterns of Al-MCM-41 and also PAM-300 (Fig. 4b, d) show that incorporation of Al into the network and also anchoring of the

Fig. 4 Low-angle XRD patterns of (a) MCM-41, (b) AM-550, (c) PAM-300

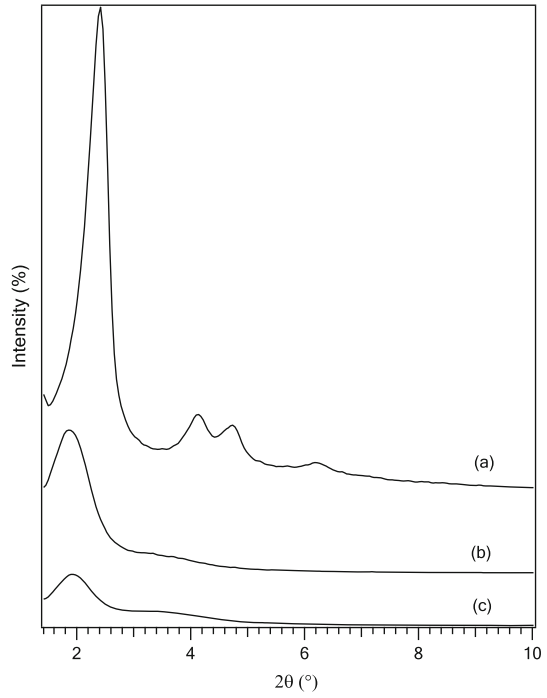
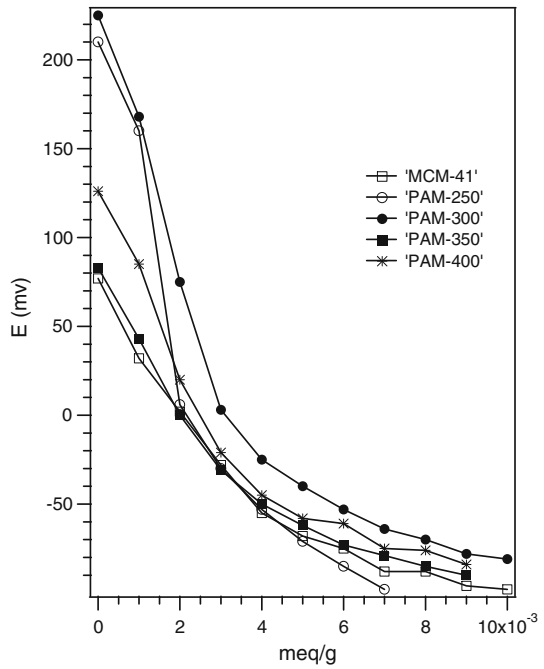


Fig. 5 Potentiometric titration of MCM-41, PAM-250, PAM-300, PAM-350, and PAM-400



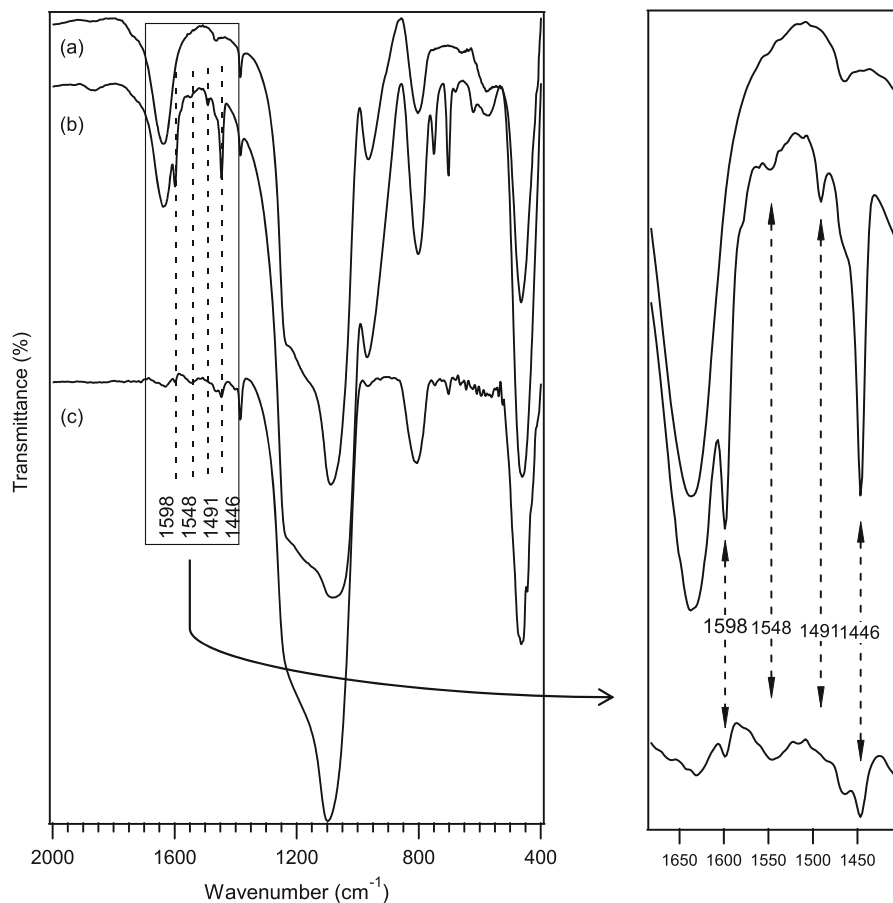


Fig. 6 FT-IR spectra of pyridine adsorption (a) PAM-300 no pyridine adsorbed, (b) pyridine adsorbed PAM-300 at ambient temperature, (c) pyridine adsorbed PAM-300 at 300 °C

perchlorate on the surface of the Al-MCM-41, affected on the intensity and width of the main peak. This is due to decrease in long-range order of hexagonal mesostructure of MCM-41.

The number of acid sites can be compared using potentiometric curves. According to this method, the initial potential electrode (E_i) shows the strength of surface acid sites and the meq of used base shows number of acid sites. The potentiometric curve of MCM-41 and PAM-300 is shown in Fig. 5. MCM-41 with the lowest potential is weak acid and PAM-300 with the greatest potential, is stronger than all. Due to highest meq of the used *n*-butyl amine per gram of the catalyst, PAM-300 has more acidic sites.

To investigate the distribution of Brønsted and Lewis acid sites on the catalyst surface, the pyridine adsorption techniques were used. Figure 6 shows the FT-IR spectra of the pyridine adsorbed PAM-300 at ambient temperature and 300 °C. The spectrum of pyridine adsorbed PAM-300 at ambient temperature (Fig. 6b) shows

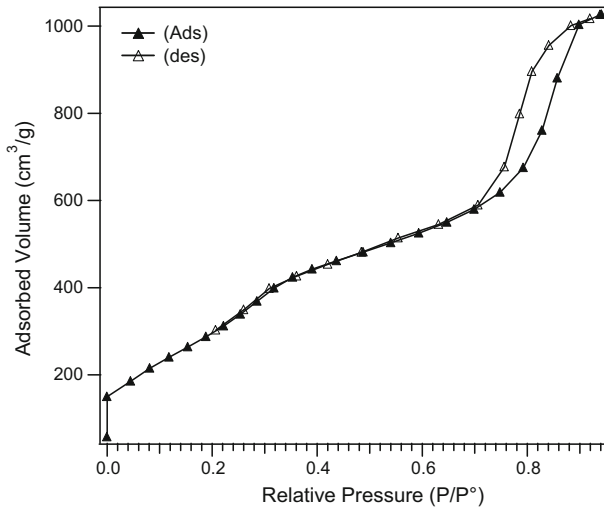


Fig. 7 N_2 adsorption–desorption isotherms of PAM-300

Table 1 Surface area of MCM-41, AM-550 and PAM-300

Entry	Catalyst	S_{BET} ($m^2\ g^{-1}$)
1	MCM-41	1505
2	Al-MCM-41	1150
3	PAM-300	847

that the peak at 1446 and $1598\ cm^{-1}$ corresponded Lewis acid sites. Weak peaks at 1543 and $1491\ cm^{-1}$ show the Brønsted acid sites. The very weak peak at $1483\ cm^{-1}$ is the combination band of pyridine bonded to both Brønsted and Lewis acid sites. Peaks of Lewis acid sites (1446 and $1598\ cm^{-1}$) are stronger than the Brønsted acid sites, which represent a higher number of Lewis acid sites. Lewis acid sites are more powerful because at high temperature, the peak of pyridine is visible (Fig. 7).

Textural properties of the catalysts were studied by surface measurement using BET method. As shown in Table 1, surface area of MCM-41 was decreased by incorporation of Al into the framework of MCM-41. Results show that impregnation of perchlorate onto the mesoporous channels of Al-MCM-41 reduces the surface area.

Figure 7 shows N_2 adsorption–desorption isotherms of PAM-300. In this isotherm, a mesoporous inflection, type IV according to IUPAC classification of adsorption isotherms [20], was observed at the relative pressure of $p/p_o = 0.2$ – 0.4 because of capillary condensation. A sharp hysteresis was observed at higher p/p_o ($p/p_o > 0.7$) due to the condensation of N_2 within voids formed by nanoparticles.

The presence of the Al content in the samples and also Si/Al molar ratios of the Al-MCM-41 and perchlorated Al-MCM-41 was investigated by means of an ICP method. The Si/Al molar ratio of AM-550 and PAM-350 was measured equal to

Table 2 Optimization of the reaction conditions for the synthesis of 2-amino-3-cyanopyridine in the presence of catalytic amount of ClO₄⁻/Al-MCM-41

Entry	Catalyst	Solvent	Temperature (°C)	Si/Al ^a	Catalyst amount (mg)	Time (min)	Yield ^b (%)
1	PAM-300	–	100	30	20	20	50
2 ^c	PAM-300	–	100	40	20	20	73
3	PAM-300	–	100	50	20	25	44
4	PAM-120	–	100	40	20	20	44
5	PAM-250	–	100	40	20	25	49
6	PAM-350	–	100	40	20	15	48
7	AM-550	–	100	40	20	80	29
8	PAM-300	–	100	40	15	20	50
9	PAM-300	–	100	40	25	30	68
10	PAM-300	–	90	40	20	60	70–80
11	PAM-300	–	110	40	20	150	60–70
12	PAM-300	–	120	40	20	90	50–60
13	PAM-300	EtOH	Reflux	40	20	720	–

^a The Si/Al molar ratio refer to the initial gel composition, mol% of the Al content for the optimized condition (for 20 mg of the PAM-300) was measured equal to 0.35 mol% relative to reactants by an ICP method

^b Isolated yield

^c Optimized conditions

61.96 and 73.45, respectively. Acid treatment of the Al-MCM-41 provokes the partial leaching of the Al from the mesoporous structure. Despite this fact, mesoporous structure of the catalyst was proved by TEM image and XRD data.

To investigate the loading amounts of perchlorate on the different PAM samples, the Cl content was determined using potentiometric titration. The wt% of ClO₄⁻ were obtained 11.2, 8, and 3.2 % for PAM-120, PAM-300, and PAM-350, respectively. Reduction from 11.2 in PAM-120 to 8 in PAM-300 may be due to decomposition of free HClO₄ on the surface. Reduction of the perchlorate content in the PAM-350 confirms rapid decomposition of perchlorate at the temperature of more than 300 °C according to literature report [21].

Catalytic activity of ClO₄⁻/MCM-41

The catalysis performance of ClO₄⁻/MCM-41 was investigated in the synthesis of 2-amino-3-cyanopyridine by the reaction of benzaldehyde (1 mmol), acetophenone (1 mmol), ammonium acetate (1.5 mmol), and malononitrile (1 mmol) under solvent-free conditions as the model reaction and results are summarized in Table 2.

In order to optimize the amount of the ClO₄⁻/Al-MCM-41, the model reaction was performed with various amounts of the catalyst and in terms of reaction time and yield of the product, 20 mg of the catalyst in the model reaction was selected as the best amount (Table 2, entries 2, 8–9).

Table 3 Four-component reaction of aldehydes, acetophenone, ammonium acetate and malononitrile in the presence of catalytic amount of $\text{ClO}_4^-/\text{Al-MCM-41}$ for the synthesis of 2-amino-3-cyanopyridine under solvent-free condition

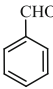
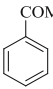
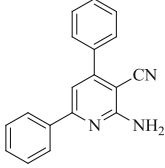
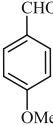
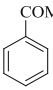
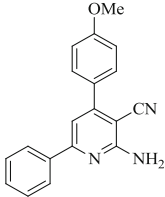
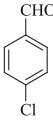
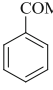
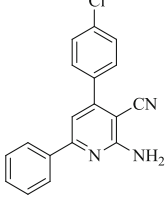
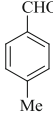
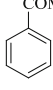
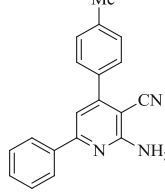
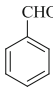
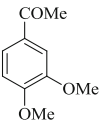
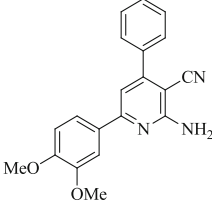
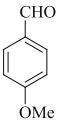
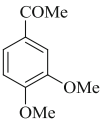
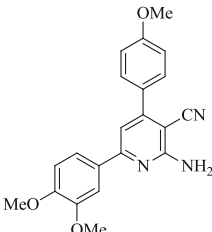
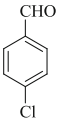
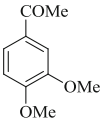
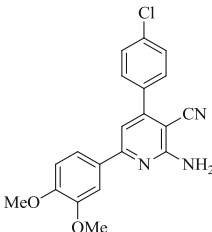
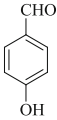
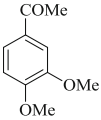
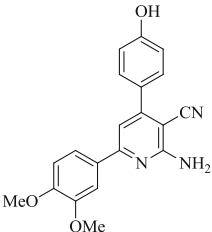
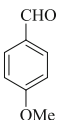
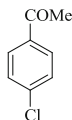
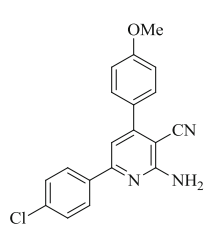
Entry	Aldehyde	Acetophenone	2-amino-3-cyanopyridine	Time (min)	Yield (%)	M.P.	
	(1)	(2)	(4)			(Found)	(Reported)
a				20	73	186	186 [4]
b				25	79	180–182	180–182 [8]
c				15	82	187–188	188–190 [4]
d				20	75	173–174	175–176 [17]
e				30	82	218–220	212–214 [18]

Table 3 continued

Entry	Aldehyde	Acetophenone	2-amino-3-cyanopyridine	Time (min)	Yield (%)	M.P.	
	(1)	(2)	(4)			(Found)	(Reported)
f				25	80	174–176	165–168 [18]
g				25	78	202–204	203–207 [18]
h				25	72	207–209	205–207 [18]
i				30	79	200–201	177 [19]

To investigate the effect of the ratio of Si/Al on the catalytic activity of ClO₄⁻/Al-MCM-41, the model reaction was performed in the presence of 20 mg of the catalyst with various Si/Al molar ratios (Table 2, entries 1–3). The results show that the molar ratio of Si/Al = 40 has the best catalytic activity.

Table 4 Reusability of $\text{ClO}_4^-/\text{Al-MCM-41}$ in the reaction of benzaldehyde, acetophenone, ammonium acetate, and malononitril

Run	Time (min)	Yield (%)
1	20	73
2	30	70
3	45	65
4	40	68 ^a

^a After calcination at 300 °C for 4 h

The effect of the calcination temperature on the catalytic activity was investigated in the model reaction in the presence of 20 mg of PAM-120, PAM-250, PAM-300, PAM-350, and PAM-400 catalysts. As shown in Table 2 (entries 1, 4–6), the results show that PAM-300 has the best catalytic activity. This result is in agreement with results of potentiometric titration of PAM samples (Fig. 5) and also decrease in the activity of PAM-350 relative to PAM-300 is in agreement with perchlorate content of PAM-300 (8 % in PAM-300 was reduced to 3.2 % in PAM-350).

To investigate the effect of temperature in the reaction, the model reaction in the presence of 20 mg PAM-300 was performed under solvent-free conditions (Table 2, entries 2, 10–12). The best temperature is 100 °C with the best yield and time for the reaction.

In order to evaluate efficiency of the $\text{ClO}_4^-/\text{Al-MCM-41}$ catalyst in the synthesis of various derivatives of 2-amino-3-cyanopyridine, the model reaction was extended to various aldehydes. Therefore, four-component reaction of aldehydes (1 mmol), acetophenone (1 mmol), ammonium acetate (1.5 mmol), and malononitrile (1 mmol) were investigated in the presence of 20 mg PAM-300 ($\text{Si}/\text{Al} = 40$) at 100 °C under solvent-free conditions and the corresponding 2-amino-3-cyanopyridine were obtained in 72–82 % yields (Table 3). The workup and the catalyst recovery are very easy. After completion of the reaction (monitored by TLC, eluent; *n*-hexane:EtOAc, 80:20), the reaction mixture was centrifuged and the catalyst was washed with EtOH (3 × 2 ml). Organic phase was collected and crystallized in ethanol to obtain pure product.

To study of the reusability of the PAM-300, the recovered catalyst from the model reaction was washed with EtOH, dried in an oven at 120 °C for 2 h, and reused in the same reaction three times. The obtained results show the moderate decrease in the catalytic activity. This may be due to blockage of active sites of the catalysts. The recycled catalyst after third run was calcined at 300 °C for 4 h. Then again, the catalyst was used in the model reaction. Decrease in the reaction time and increase in the yield, demonstrate blocking of holes in previous reaction (Table 4). The FT-IR vibrational peaks of various functional groups of organic material in the spectrum of reused catalyst confirm blocking of surface on the catalyst. However, ICP analysis of Al content and also analysis of perchlorate confirms that there is not any leaching in the reaction media.

Conclusions

In this work, we prepared Al-MCM-41 with various Si/Al molar ratio. To promotion of the catalytic activity, Al-MCM-41 was treated with perchloric acid. It was concluded that acid treatment of the Al-MCM-41 by perchloric acid promotes its catalytic activity. We also investigated parameters such as Si/Al mol ratio and temperature of calcination that have notable effects on the activity of the catalyst. In order to characterize the catalyst, various techniques such as SEM, TEM, FT-IR, potentiometric titration, pyridine adsorption, and nitrogen adsorption–desorption have been applied to investigate the structure and catalytic activity of the catalyst. To testify the activity of the prepared catalyst, synthesis of 2-amino-3-cyanopyridines was performed in the presence of a catalytic amount of perchlorated Al-MCM-41 as an efficient and reusable catalyst. High yields, simple operation, non-toxic catalyst and solvents, short reaction time, and minimum pollution of the environment are some other advantages of this method.

References

1. M.D. Hill, *Chem. -A Eur. J.* **16**, 12052–12062 (2010)
2. N. Patel, *J. Sci., Islamic Republic of Iran* **21**, 121–129 (2010)
3. H.M. Hosni, M.M. Abdulla, *Acta Pharmaceutica* **58**, 175–186 (2008)
4. R. Gupta, A. Jain, M. Jain, R. Joshi, *Bull. Korean Chem. Soc.* **31**, 3180–3182 (2010)
5. A. Hantzsch, *Justus Liebigs Annalen der Chemie* **215**, 1–82 (1882)
6. H. Adibi, H.A. Samimi, M. Beygzadeh, *Catal. Commun.* **8**, 2119–2124 (2007)
7. S. Ko, M.N.V. Sastry, C. Lin, C.-F. Yao, *Tetrahedron Lett.* **46**, 5771–5774 (2005)
8. H. Sheibani, K. Saidi, M. Abbasnejad, A. Derakhshani, I. Mohammadzadeh, *Arab. J. Chem.* (2011)
9. J. Li, P. He, C. Yu, *Tetrahedron* **68**, 4138–4144 (2012)
10. T. Ram Reddy, G. Rajeshwar Reddy, L. Srinivasula Reddy, S. Jammula, Y. Lingappa, R. Kapavarapu, C.L. Meda, K.V. Parsa, M. Pal, *Eur. J. Med. Chem.* **48**, 265–274 (2012)
11. J. Tang, L. Wang, Y. Yao, L. Zhang, W. Wang, *Tetrahedron Lett.* **52**, 509–511 (2011)
12. M. Abdollahi-Alibeik, M. Pouriayevali, *Reac. Kinet. Mech. Cat.* **104**, 235–248 (2011)
13. M. Abdollahi-Alibeik, N. Sadeghi-Vasafi, *Reac. Kinet. Mech. Cat.* **112**, 511–525 (2014)
14. M. Abdollahi-Alibeik, G. Ahmadi, *Res. Chem. Intermed.* doi:[10.1007/s11164-014-1883-3](https://doi.org/10.1007/s11164-014-1883-3)
15. M. Abdollahi-Alibeik, A. Moaddeli, *RSC Adv.* **4**, 39759–39766 (2014)
16. M. Abdollahi-Alibeik, A. Rezaeipoor-Anari, *Cat. Sci. Tech.* **4**, 1151–1159 (2014)
17. S. Khaksar, A. Rouhollahpour, S.M. Talesh, *J. Fluorine Chem.* **141**, 11–15 (2012)
18. A. Abadi, O. Al-Deeb, A. Al-Afify, H. El-Kashef, *Il Farmaco*, **54**, 195–201 (1999)
19. F. Shi, S. Tu, F. Fang, T. Li, *Arkivoc* **1**, 137–142 (2005)
20. K. Sing, D. Everett, R. Haul, L. Moscou, L. Pierotti, J. Rouquérol, T. Siemieniowska, *Pure Appl. Chem* **57**, 603–619 (1985)
21. M.P. Henderson, V.I. Miasek, T.W. Swaddle, *Can. J. Chem.* **49**, 317–324 (1971)